

This is in qualitative accord with the electron screening mechanism since electrical resistivity<sup>11</sup> increases rapidly as  $T$  decreases and, for  $x = \frac{1}{3}$ , has already reached relatively high values ( $10^2 - 10^3 \Omega \text{ cm}$ ) at  $150^\circ\text{K}$  whereas for  $x = 0.1$  the resistivity at  $150^\circ\text{K}$  is only  $\sim 10^{-2} \Omega \text{ cm}$  and does not reach values  $10^2 - 10^3 \Omega \text{ cm}$  until  $T \lesssim 20^\circ\text{K}$ .

In conclusion we have observed an unusual temperature dependence of QS in  $1T\text{-Fe}_{0.1}\text{Ta}_{0.9}\text{S}_2$  which can be understood in terms of a temperature-modulated contribution from a local lattice distortion. The distinctive temperature modulation of this distortion is produced by a stricitive interaction with the continuous LS-HS magnetic transition of  $\text{Fe}^{2+}$  in this material and allows us for the first time to observe a magnetic modulation of a lattice EFG. The onset of CDW instability is also clearly observable in the QS data.

We thank M. Robbins for reducing  $^{57}\text{Fe}_2\text{O}_3$  to  $^{57}\text{Fe}$  metal, J. V. Waszczak for providing the crystals of  $^{57}\text{Fe}$ -doped  $\text{TaS}_2$ , and W. F. Brinkman for helpful discussions.

<sup>1</sup>P. Jena, Phys. Rev. Lett. **36**, 418 (1976).

<sup>2</sup>D. R. Torgeson and F. Borsa, Phys. Rev. Lett. **37**, 956 (1976).

<sup>3</sup>K. Nishiyama, F. Dimmling, Th. Kornrumpf, and D. Riegel, Phys. Rev. Lett. **37**, 357 (1976).

<sup>4</sup>J. A. Wilson, F. J. DiSalvo, and S. Mahajan, Adv. Phys. **24**, 117 (1975).

<sup>5</sup>W. L. McMillan, Phys. Rev. B **12**, 1187 (1975), and **14**, 1496 (1976).

<sup>6</sup>M. Eibschütz, M. E. Lines, and F. J. DiSalvo, Phys. Rev. B **15**, 103 (1977).

<sup>7</sup>Mössbauer data were obtained with a conventional constant-acceleration Doppler spectrometer. The source was  $\text{Co}^{57}$  in Pd. The absorber was the same as in Ref. 6. For a typical spectrum see Fig. 2 of that paper.

<sup>8</sup>J. S. Griffith, *Transition Metal Ions* (Cambridge Univ. Press, Cambridge, England, 1961).

<sup>9</sup>A. Vasquez, T. Butz, E. Saitovitch, and A. Lerf, in Proceedings of the Fourth International Conference on Hyperfine Interactions, Madison, New Jersey, 1977 (to be published), paper No. 6.16, p. 204.

<sup>10</sup>F. J. DiSalvo, J. A. Wilson, B. G. Bagley, and J. V. Waszczak, Phys. Rev. B **12**, 2202 (1975).

<sup>11</sup>F. J. DiSalvo, J. A. Wilson, and J. V. Waszczak, Phys. Rev. Lett. **36**, 885 (1976).

## Zero-Temperature Spin Dynamics of Model Spin-Glass Hamiltonians

W. Y. Ching, K. M. Leung, and D. L. Huber

*Department of Physics, University of Wisconsin, Madison, Wisconsin 53706*

(Received 18 July 1977)

Computer modeling techniques are used to obtain information about the spin dynamics of model spin-glass Hamiltonians in the zero-temperature limit. The density of states and dynamic structure factor are computed numerically for the Edwards-Anderson and Mattis models with Heisenberg interactions. We find no evidence for spin-wave modes in the former; the latter shows spin-wave behavior characteristic of a disordered  $XY$  model.

The nature of the low-lying excitations in spin-glass alloys is a question of considerable importance in the interpretation of thermodynamic data. In this Letter we report the results of a numerical analysis of the zero-temperature dynamic response of two models which have certain thermal and magnetic properties that are believed to be characteristic of spin-glasses. We calculate the density of states and the dynamic structure factor for the classical Edwards-Anderson (E-A)<sup>1</sup> and Mattis<sup>2</sup> models with Heisenberg interactions between nearest neighbors. The dynamic response of the Mattis model in the zero-temperature limit is found to be qualitatively similar to that of the  $XY$  model, which in three dimensions is described by linear spin-wave the-

ory. In contrast, we find no evidence of spin waves in the E-A model.

In its simplest form the E-A model consists of a Heisenberg Hamiltonian

$$\mathcal{H} = \frac{1}{2} \sum_{i,j} J_{ij} \vec{S}_i \cdot \vec{S}_j \quad (1)$$

with a Gaussian distribution for the exchange integrals  $J_{ij}$ . We specialize to nearest-neighbor interactions between classical spins of unit magnitude on a simple cubic lattice. The distribution of the  $J_{ij}$  has a mean value of zero and a root-mean-square width  $\Delta J$ . In our determination of the density of states we follow a procedure similar to that of Walker and Walstedt in their numerical analysis of a spin-glass alloy with a Ruder-

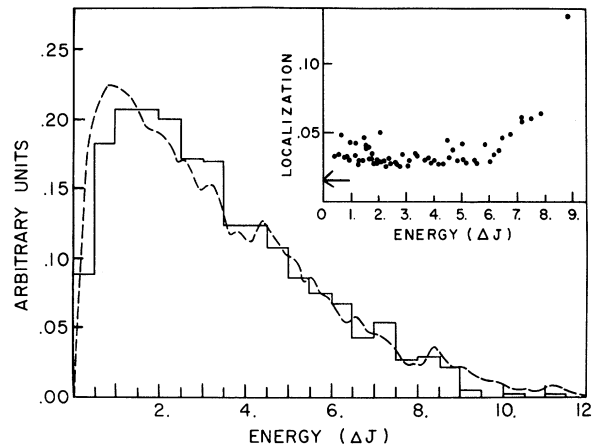


FIG. 1. Density of states for the E-A model. Histogram is the average over twelve configurations for a  $4 \times 4 \times 4$  array. Inset shows the localization indices (Ref. 3) for one configuration. The arrow denotes the value  $\frac{1}{64}$ , the index of a delocalized state with equal amplitude on all sites. The broken curve is the density of states obtained by equation-of-motion methods for a single configuration of a  $10 \times 10 \times 10$  array, normalized to the same area as the histogram.

man-Kittel-Kasuya-Yosida (RKKY) interaction.<sup>3</sup> For a given set of exchange integrals we calculate the equilibrium configuration of spins by minimizing the energy. The normal modes are determined by linearizing the equations of motion for the spins, treating the deviations from the equilibrium orientation as small parameters. Assuming a harmonic time dependence we obtain a dynamical matrix whose eigenvalues are the energies of the normal modes. Our results for the normalized density of states of  $4 \times 4 \times 4$  arrays with periodic boundary conditions are shown in Fig. 1, where we have plotted the values obtained by averaging over twelve configurations of the  $J_{ij}$ . Following Ref. 3 we can use the eigenvectors of the dynamical matrix to calculate the localization indices of the various modes, which are plotted in the inset. A comparison of Fig. 1 with the corresponding data in Ref. 3 indicates that the densities of states are qualitatively similar. However the localization indices of the E-A model are much less energy dependent than the indices of the RKKY model where only the low-energy modes are significantly delocalized. We have also calculated the zero-temperature susceptibility with the result  $\chi(0) = (0.45 \pm 0.03)/\Delta J$  which is in agreement with the zero-temperature extrapolation of our Monte Carlo data reported earlier,<sup>4</sup>  $\chi(0) = (0.45 \pm 0.05)/\Delta J$ .

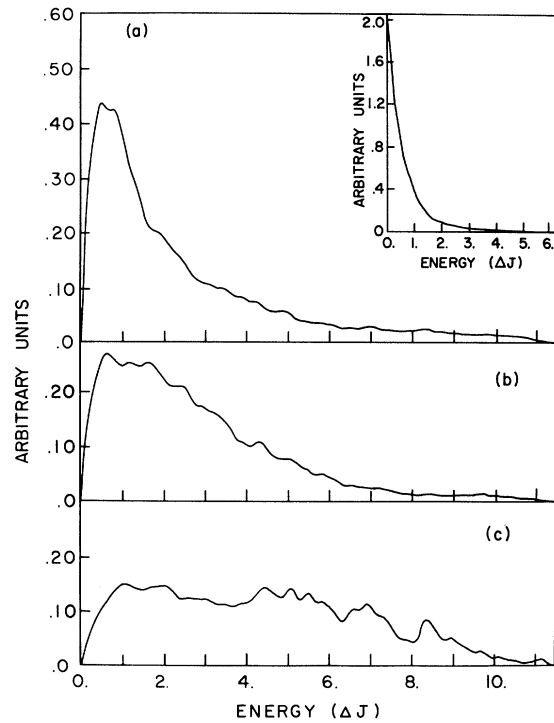


FIG. 2. Dynamic structure factor,  $S(\vec{k}, E)$ , for the E-A model, single configuration,  $10 \times 10 \times 10$  array: (a)  $\vec{k} = (\pi/10)(1, 1, 1)$ ; (b)  $\vec{k} = (2\pi/5)(1, 1, 1)$ ; (c)  $\vec{k} = \pi(1, 1, 1)$ . All curves are normalized to the same area. Inset shows  $S(\vec{k}, E)/E$  for  $\vec{k} = (\pi/10)(1, 1, 1)$ .

An important question is whether any of the low-frequency modes can be identified as spin waves which we define as delocalized modes characterized by a dispersion relation  $E_k = f(k)$ ,  $k$  being the wave vector.<sup>5-7</sup> In order to study this aspect of the problem we have used equation-of-motion techniques similar to those developed by Alben and Thorpe<sup>8</sup> to calculate the dynamic structure factor  $S(\vec{k}, E) = \frac{1}{3}[S_{xx}(\vec{k}, E) + S_{yy}(\vec{k}, E) + S_{zz}(\vec{k}, E)]$  for  $10 \times 10 \times 10$  arrays. This was done by projecting  $\vec{S}(\vec{k}) = \sum_j \exp(i\vec{k} \cdot \vec{r}_j) \vec{S}_j$  onto the local spin deviations and then determining the dynamic correlation functions by expressing  $\langle S_\alpha(\vec{k}, t) S_\alpha(-\vec{k}, 0) \rangle$  as a linear combination of the Green's functions associated with the local variables. The differential equations for the Green's functions were integrated forward in time out to  $t = 20/\Delta J$  with an exponential damping factor,  $\exp(-0.15t/\Delta J)$ .

Our data for  $\vec{k} = \pi(1, 1, 1)$ ,  $(2\pi/5)(1, 1, 1)$ , and  $(\pi/10)(1, 1, 1)$  are shown in Fig. 2. It is evident that as  $k$  decreases the intensity builds up at low frequencies, a result consistent with the fact that  $\vec{S}(\vec{k} = 0)$  is a constant of the motion. From Fig. 2 it would appear the the peak in  $S(\vec{k}, E)$  for

$\vec{k} = (\pi/10)(1, 1, 1)$  is in fact the spin-wave mode mentioned earlier. We do not believe that this is the case. The equation-of-motion formalism constrains  $S(k, E=0)$  to be zero.<sup>8</sup> The rapid decrease in  $S(k, E)$  below  $0.5\Delta J$  is consistent with this constraint and the finite interval of integration. This interpretation is supported by a plot of the function  $S(k, E)/E$  shown in the inset which decreases monotonically with increasing  $E$ . We have also used equation-of-motion techniques to calculate the density of states. Our results are shown as the dashed curve in Fig. 1, which is in good agreement with the histogram. Unfortunately because of the finite size of the arrays and the finite interval of integration we were not able to determine if the density of states remains finite in the zero temperature limit. Thus we cannot rule out the existence of long-wavelength ( $k \ll \pi/10$ ) spin-wave modes with energies  $\ll \Delta J$  which give rise to an  $E^2$  dependence in the density of

states at very low energies. However if such modes exist they do not dominate the line shape. We have used numerical techniques to calculate  $\langle E_k^2 \rangle$  and  $\langle E_k^4 \rangle$ , the second and fourth moments of the normalized line-shape function. As  $k \rightarrow 0$  we find that  $\langle E_k^4 \rangle \gg \langle E_k^2 \rangle^2$  rather than  $\langle E_k^4 \rangle = \langle E_k^2 \rangle^2$ , which would be the case if the line shape consisted only of  $\delta$  functions at energies  $E = \pm \langle E_k^2 \rangle^{1/2}$ .

The dynamics of the classical E-A model at zero temperature is appreciably different from the Mattis model. The latter is characterized by the Hamiltonian

$$\mathcal{H} = -\frac{1}{2} \sum_{i,j} J_{ij} \xi_i \xi_j \vec{S}_i \cdot \vec{S}_j, \quad (2)$$

where  $J_{ij}$  is translationally invariant and the  $\xi_i$  are random variables taking on the values  $\pm 1$ . As shown by Sherrington,<sup>9</sup> Eq. (2) can be expanded in a Holstein-Primakoff series about the classical ground state,  $\vec{S}_i = S \xi_i \vec{\tau}$ ,  $\vec{\tau}$  being a unit vector of arbitrary direction. The term bilinear in the boson variables takes the form

$$\mathcal{H} = (\sum_{j,k} J_{kj}) S \sum_i a_i^\dagger a_i - S \sum_{i,j} J_{ij} \{ a_i^\dagger a_j (1 + \xi_i \xi_j) / 2 - \frac{1}{2} (a_i^\dagger a_j^\dagger + a_i a_j) (1 - \xi_i \xi_j) / 2 \}, \quad (3)$$

where the  $a_i$  and  $a_i^\dagger$  are Bose operators with the standard commutation relations. Our interest here is in the special case where the mean value of the  $\xi_i$  is zero so that there is no overall magnetic moment. In this limit (3) is equivalent to the magnon Hamiltonian of a disordered XY model, the ordered counterpart consisting of the terms without the factor  $\xi_i \xi_j$ .<sup>10</sup>

In order to determine the effects of disorder on the dynamical properties we have made use of equation-of-motion techniques to calculate the density of states and dynamic structure factor for  $12 \times 12 \times 12$  arrays with nearest-neighbor interactions and periodic boundary conditions. Our results for the density of states are shown in Fig. 3 where for comparison we have plotted the density of states of the simple-cubic XY model normalized to the same area. The distribution of modes in the disordered system qualitatively resembles the distribution for the XY model. This resemblance carries over into the dynamic structure factor shown in Fig. 4 for  $\vec{k} = \pi(1, 1, 1)$ ,  $(\pi/2)(1, 1, 1)$ , and  $(\pi/6)(1, 1, 1)$ . In each case there is a peak in the spectrum in the vicinity of the energy of the spin-wave mode in the XY model which is given by  $E_k = 6JS(1 - \cos k)^{1/2}$  for  $\vec{k}$  along [111]. It is apparent that there is only a slight renormalization of the spin-wave velocity at long wavelengths. However, even at  $(\pi/6)(1, 1, 1)$  the half-width of the peak is still greater than the

“instrumental width,”  $0.4JS$  (full width at half-maximum), that is introduced by the exponential cutoff in the integration.

We speculate that the difference in the spin dynamics of the two models is a consequence of the fact that (3) can be regarded as a disordered spin-wave Hamiltonian<sup>9</sup> whereas there is no obvious ordered counterpart to the E-A model. An intriguing question is whether the RKKY model

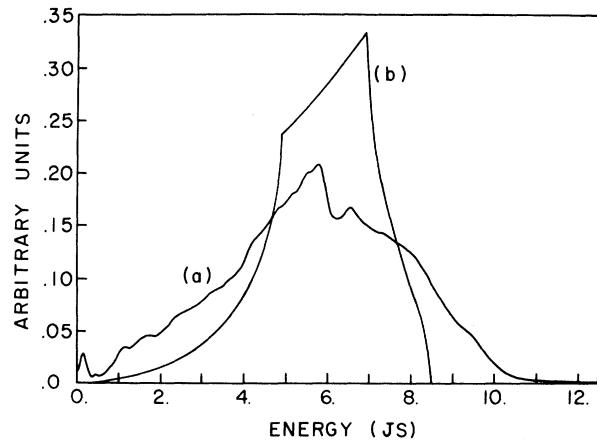


FIG. 3. Curve *a*, density of states for the Mattis model,  $12 \times 12 \times 12$  array, average over three configurations; curve *b*, density of states of the simple-cubic XY model. Both curves have the same area.

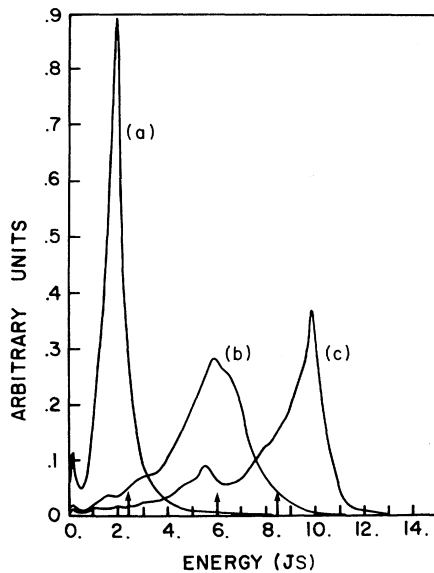


FIG. 4. Dynamic structure factor for the Mattis model,  $12 \times 12 \times 12$  array, single configuration; curve a,  $\vec{k} = (\pi/6)(1, 1, 1)$ ; curve b,  $\vec{k} = (\pi/2)(1, 1, 1)$ ; curve c,  $\vec{k} = \pi(1, 1, 1)$ . All curves are normalized to the same area. Arrows show the corresponding spin-wave peaks for the XY model.

Hamiltonian of Ref. 3 resembles either of the two models considered here. This problem is under investigation and the results will be reported elsewhere.

This work was supported by the National Science Foundation under the Grant No. DMR-77-01057. We would like to thank the authors of Refs. 3 and 7 for providing us with preprints of

their work.

<sup>1</sup>S. F. Edwards and P. W. Anderson, *J. Phys. F* **5**, 965 (1975).

<sup>2</sup>D. C. Mattis, *Phys. Lett.* **56A**, 421 (1976).

<sup>3</sup>L. R. Walker and R. F. Walstedt, *Phys. Rev. Lett.* **38**, 514 (1977).

<sup>4</sup>W. Y. Ching and D. L. Huber, in *Magnetism and Magnetic Materials—1973*, AIP Conference Proceedings No. 34, edited by J. J. Becker and G. H. Lander (American Institute of Physics, New York, 1976), p. 370. Similar agreement is obtained for the specific heat of the classical E-A model which has the value  $Nk_B$  in the limit  $T = 0$  [W. Y. Ching and D. L. Huber, *Phys. Lett.* **59A**, 383 (1976)].

<sup>5</sup>S. F. Edwards and P. W. Anderson, *J. Phys. F* **6**, 1927 (1976).

<sup>6</sup>D. L. Huber and W. Y. Ching, in *Amorphous Magnetism II*, edited by R. A. Levy and R. Hasegawa (Plenum, New York, 1977), p. 39.

<sup>7</sup>B. I. Halperin and W. M. Saslow, *Phys. Rev. B* (to be published). These authors mention that the effective spin-wave stiffness constant may be zero, which would be consistent with our findings for the E-A model.

<sup>8</sup>R. Alben and M. F. Thorpe, *J. Phys. C* **8**, L275 (1975); M. F. Thorpe and R. Alben, *J. Phys. C* **9**, 2555 (1976). Our analysis is more complicated than theirs in that we have to integrate coupled equations involving Green's functions of the type  $\langle\langle a^\dagger(t); a^\dagger(0) \rangle\rangle$ , as well as  $\langle\langle a(t); a^\dagger(0) \rangle\rangle$ .

<sup>9</sup>D. Sherrington, *J. Phys. C* **10**, L7 (1977). In this Letter it is suggested that it may be more appropriate to regard the Mattis Hamiltonian as a model spin-magnet.

<sup>10</sup>J. S. Semura and D. L. Huber, *Phys. Rev. B* **7**, 2154 (1973).